Advances in Materials Technology for Fossil Power Plants
Proceedings from the Eighth International Conference
October 11–14, 2016, Albufeira, Algarve, Portugal
https://doi.org/10.31399/asm.cp.am-epri-2016p0458

EFFECT OF STRESS AND STRAIN ON MICROSTRUCTURAL CHANGES DURING LONG-TERM CREEP IN T91 STEEL

Kota Sawada, Toru Hara, Hideaki Kushima, Kazuhiro Kimura, Masaaki Tabuchi
National Institute for Materials Science, Tsukuba, Ibaraki 305-0047, Japan

ABSTRACT

In order to clarify the effect of stress and strain on microstructural changes during creep for T91 steel, creep interrupted tests were performed at 600°C for 10000h, 20000h, 30000h, 50000h and 70000h. The steel studied was T91 steel with high Ni content (0.28mass%) in the range of specification. Changes of dislocation structure and precipitates distributions were observed for the grip and gauge portions of creep interrupted samples. The subgrain size gradually increased with increasing creep time up to 50000h in both the grip and gauge portions. However, the subgrain size abruptly increased after 50000h in the gauge portion as compared with the grip portion. Decrease in dislocation density inside subgrain was promoted in the gauge portion as compared with the grip portion. The size of $M_{23}C_6$ gradually increased with increasing creep time up to 50000h in both the grip and gauge portions. The increase in $M_{23}C_6$ size was accelerated after 50000h in the gauge portion as compared with the grip portion. The Z phase formation was promoted in the gauge portion as compared with the grip portion. The number density of all kinds of particles gradually decreased with increasing creep time in the gauge and grip potions. After 50000h, the number density rapidly decreased in the gauge portion as compared with the grip portion.

INTRODUCTION

Thermal power plants are still supplying large amounts of electric power in Japan at the moment. For the coal-fired power plants, the USC and A-USC power plants are very important because high efficiency power plants are strongly needed to suppress CO_2 emissions in Japan. The safe operation of USC power plants is also concern in terms of stable power supply. The Grade 91 steels are widely used for boiler components of USC power plants. However, review of allowable stresses of Grade 91 steels is still concern since it has been reported that the creep strength of Grade 91 steel degraded in the long-term in some cases [1, 2].

In order to make clear the mechanism of creep strength degradation of Grade 91 steels, process of microstructural changes during long-term creep should be understood. For example, quantitative evaluation of microstructural changes can be useful for prediction of metal temperature of actual components because microstructural changes are sensitive to temperatures. It is predicted that stress of actual component is much lower than that of creep testing. Therefore, it is needed to know the effect of stress and strain on microstructural changes during creep to predict metal temperature of component based on process of microstructural changes obtained from crept samples.

In this paper, we investigated the effect of stress and strain on microstructural changes during long-term creep, focusing on the subgrain size, dislocation density, particle size and number density of particles in T91 steel.

EXPERIMENTAL PROCEDURES

The material studied was ASME T91 steel. The chemical composition and heat treatment condition is listed in Table 1. The Ni content is relatively high in the range of specification. We already reported that the long-term creep strength was lower in high Ni steel than in low Ni one [3], meaning that the material studied is weak heat. Creep interrupted tests were performed at 600°C under 70MPa. The interrupted time was 10000h, 20000h, 30000h, 50000h and 70000h. The time to rupture was 80736.8h. The samples for microstructural observations were cut from the gauge and grip portions of crept specimens. The microstructures were observed using a transmission electron microscopy (TEM), a scanning electron microscope (SEM) and a transmission electron microscopy–energy dispersive spectroscopy (STEM–EDS). The subgrain size, dislocation density and particle size were measured on TEM micrographs. The number density of precipitates was measured on SEM micrographs. The results of microstructural changes for the gauge portion were already reported [4].

Table 1 : Chemical composition (mass%) and heat treatment condition of the steel examined.

C	Si	Mn	P	S	Ni	Cr	Mo	V
0.09	0.29	0.35	0.009	0.002	0.28	8.70	0.90	0.22

Nb	N	Al	Normalizing	Tempering
0.072	0.044	0.001	1050°C, 10min A.C.	765°C, 30min A.C.

RESULTS and DISCUSSION

Creep strength and hardness change during creep

Figure 1 shows the creep strength of the steel studied [4]. The creep strength abruptly degraded in the long-term at 550°C, 600°C and 650°C. The creep strength degradation in the long-term was very clear at 600°C. The condition (600°C, 70MPa) of creep interrupted tests corresponds to the condition at which the creep strength degradation occurs. Hardness change is shown in Fig.2.

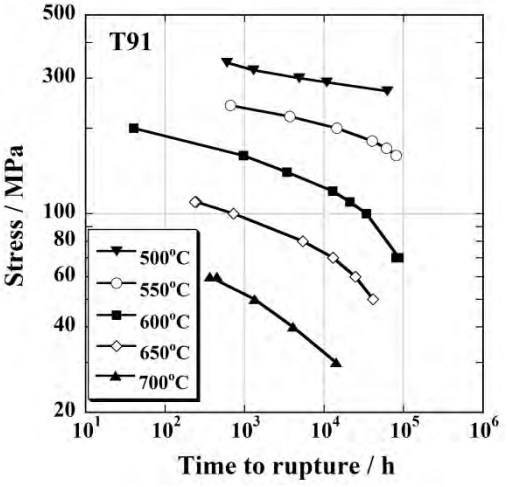

Figure 1 : Creep strength of the steel studied.

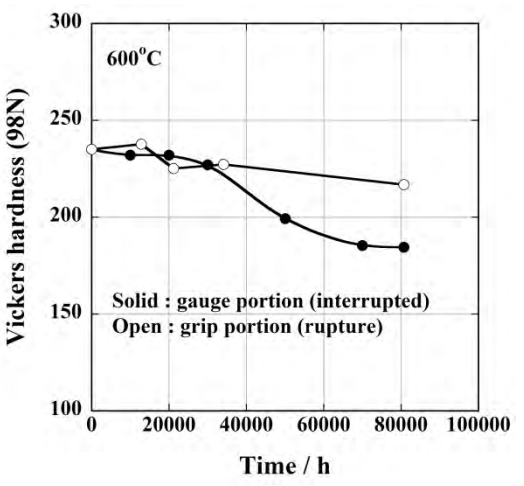

Figure 2 : Hardness change during creep.

The hardness of gauge portion was obtained from the interrupted samples. On the other hand, the hardness of grip portion was measured in creep ruptured samples. The hardness of grip portion gradually decreased with increasing creep time. The hardness of gauge portion gradually decreased up to 30000h in the same way as the grip portion, and then rapidly dropped up to creep rupture. It is expected that microstructural changes abruptly occurs after 30000h in the gauge portion.

Change in dislocation structure

Figure 3 shows the change in martensitic structure during creep in the grip and gauge portions. The change in subgrain size in the grip portion was not large even after creep rupture. The increase in subgrain size was small after 50000h in the gauge portion. However, the subgrain size abruptly increased after creep rupture in the gauge portion. The stress or strain strongly promoted the increase in subgrain size during creep.

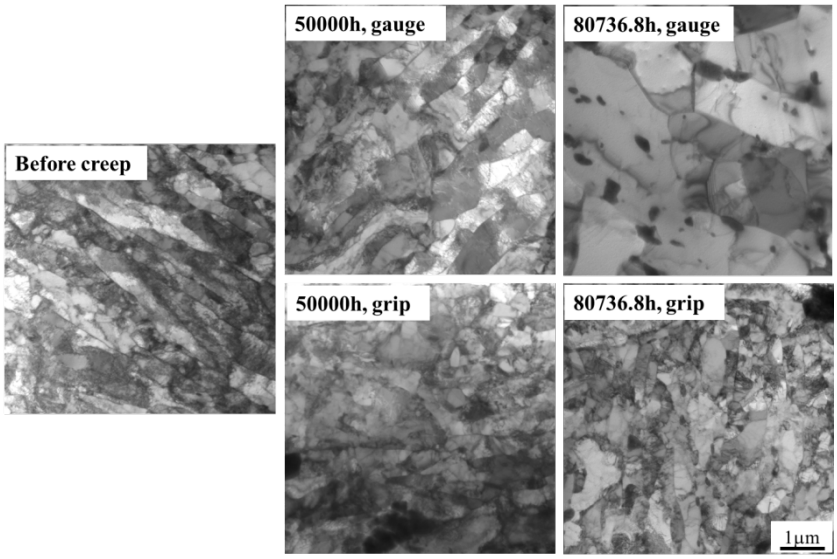

Figure 3 : Change in martensitic structure during creep.

The mean subgrain size is plotted against creep time in Fig.4. The mean subgrain size gradually increased with increasing creep time in the grip and gauge portions. In the gauge portion, the mean subgrain size rapidly increased after 70000h although the increase in mean subgrain size was small after 70000h in the grip portion. Figure 5 demonstrates the change in dislocation density inside subgrain during creep. The dislocation density gradually decreased with increasing creep time in the grip and gauge portions. In the gauge portion, the dislocation density abruptly decreased after 70000h. On the other hand, the decrease in dislocation density was very small after 70000h in the grip portion. The changes in subgrain size and dislocation density were strongly promoted in the gauge portion at the later stage of creep process as shown in Fig4 and Fig.5. This indicates that strain accumulation can strongly relate with the change in subgrain size and dislocation density [5, 6]. The hardness abruptly decreased after 30000h in the gauge portion as shown in Fig.2. It can be predicted that the effect of dislocation density and subgrain size on hardness is not so large because the abrupt changes in dislocation density and subgrain size occurred after 70000h in the gauge portion.

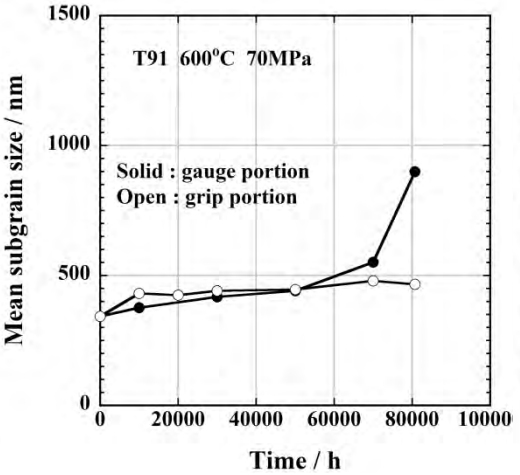

Figure 4 : Change in subgrain size during creep.

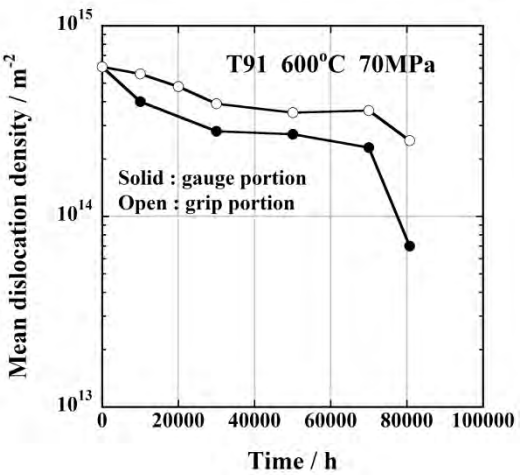

Figure 5 : Change in dislocation density during creep.

Changes in precipitate distribution and particle size

Figure 6 demonstrates elemental maps of carbon extracted replica in the grip and gauge portions. Red, blue, green, yellow and white color means $M_{23}C_6$, V-rich MX, Nb-rich MX, Laves phase and Z phase particles, respectively. It seemed that the size of $M_{23}C_6$ particle gradually increased during creep in the grip and gauge portions. The size of $M_{23}C_6$ particle seems to be much larger in the gauge portion than in the grip portion after creep rupture. In the gauge portion, the Z phase particles were clearly observed after creep as compared with the grip portion. Many of MX particles were disappeared after creep in the gauge portion. The Laves phase particles were also observed in the grip portion after creep although no Laves phase particles were conformed in the gauge portion. The presence of Laves phase may depend on observation area because the number of Laves phase particles is not so high.

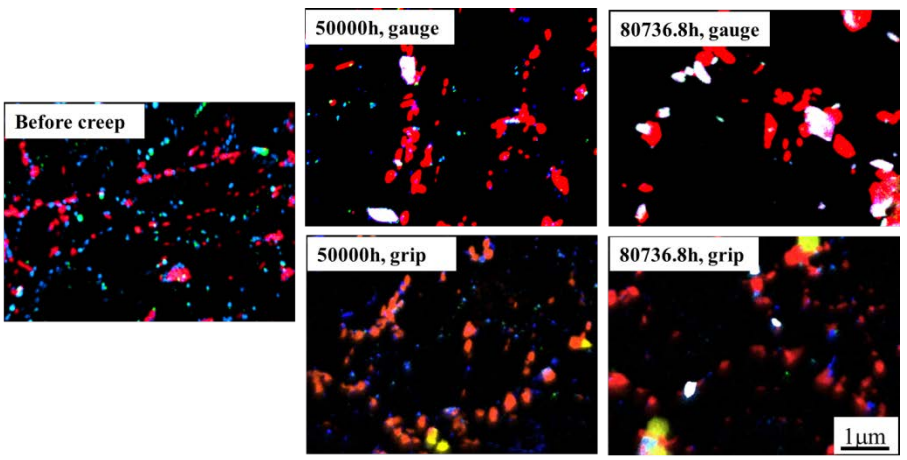

Figure 6 : Results of elemental mapping of Cr, V, Nb and Mo for carbon extracted replica Red : $M_{23}C_6$, Blue : V-rich MX, Green : Nb-rich MX, Yellow : Laves phase, White : Z phase

Figure 7 shows the relationship between the mean size of $M_{23}C_6$ particles and creep time. The mean size of $M_{23}C_6$ particles gradually increased with increasing creep time in the grip and gauge portions. However, the mean size of $M_{23}C_6$ particles rapidly increased after 50000h in the gauge portion as compared with the grip portion. The rapid increase in the mean size of $M_{23}C_6$ particles occurred at the later stage of creep process, indicating that strain accumulation promoted the $M_{23}C_6$ coarsening.
The $M_{23}C_6$ coarsening in high Cr ferritic steels can be expressed by Ostwald-ripening equation [7-9].

$$r^3 - r_0^3 = kt \tag{1}$$

where r and r_0 are ,the mean particle radius at time t and 0, respectively, k is the rate constant. Figure 8 demonstrates the relationship between the value of $(r^3 - r_0^3)$ and time t. The coarsening of $M_{23}C_6$ in the grip portion was expressed by the equation (1). On the other hand, the coarsening of $M_{23}C_6$ in the gauge portion was deviated from the equation (1) after 50000h. In the case of $M_{23}C_6$ coarsening in the gauge portion, the Ostwald-ripening equation should be modified, considering the effect of strain accumulation on the coarsening. Taneike et al. proposed modified Ostwald-ripening equation for MX coarsening in 12Cr steel, introducing the effective diffusion coefficient consists of the lattice diffusion coefficient and dislocation diffusion coefficient [10]. They reported that moving dislocations during creep strongly promoted diffusion, leading to acceleration of MX coarsening. Many of $M_{23}C_6$ particles are located on lath, block, packet and prior austenite grain boundaries. However, there is possibility that dislocations inside lath can move and interact with the lath and block boundaries. This indicates that the dislocation diffusion by the moving dislocations can promote the $M_{23}C_6$ coarsening during creep.

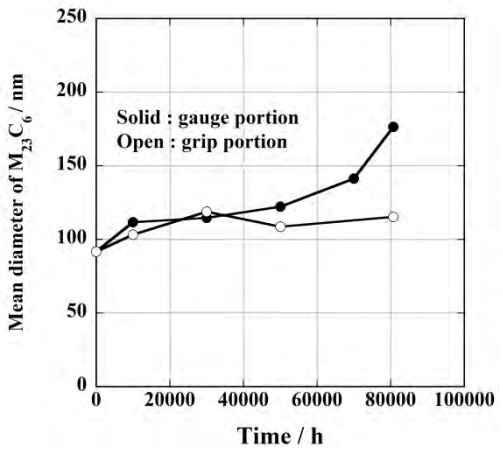

Figure 7 : Relationship between mean diameter of $M_{23}C_6$ and creep time.

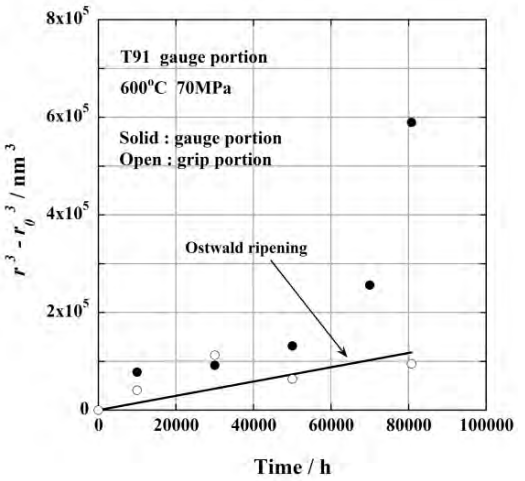

Figure 8 : Comparison between experimental data and Oswald-ripening.

The MX particles disappear during creep due to the Z phase formation as shown in Fig.6. Therefore, it is difficult to discuss the coarsening behavior of MX particles during creep based on the Ostwald-ripening mechanism. Figure 9 shows changes in the number densities of MX particles and Z phase particles during creep [11]. The number density was measured on carbon extracted replica. The number density of Z phase particles gradually increased with increasing

creep time in the grip and gauge portions. After 30000h, the number density of Z phase particles was higher in the gauge portion than in the grip portion. The number density of MX particles gradually decreased with increasing creep time in the grip and gauge portions. The number density of MX particles abruptly decreased after 30000h in the gauge portion as compared with the grip portion. It is expected that the stress or strain promoted the Z phase formation during creep.

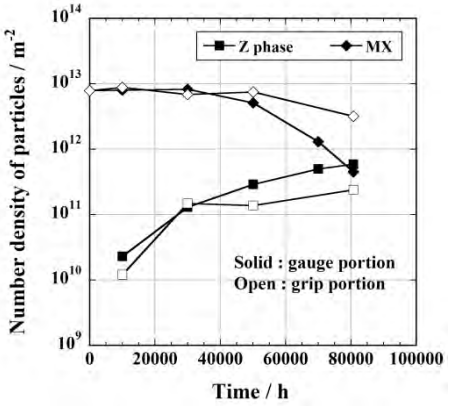

Figure 9 : Change of number density of MX and Z phase particles during creep.

Figure 10 shows the SEM micrographs of as received and creep ruptured sample. Black and grey particles were observed before and after creep. It was confirmed by EDS that the black and grey particles mainly contained Cr and V, respectively. The black and grey particles can be MX and $M_{23}C_6$, respectively. However, the black particles can be MX or Z phase in the case of creep ruptured sample since the Z phase also contains V. After creep rupture, the number of particles apparently decreased in the gauge portion as compared with that before creep. It seems that the number of particles is higher in the grip portion than in the gauge portion after creep rupture. The total number density of particles such as $M_{23}C_6$, MX, Laves phase and Z phase was evaluated in the grip and gauge portions, using the SEM micrographs shown in Fig.10.

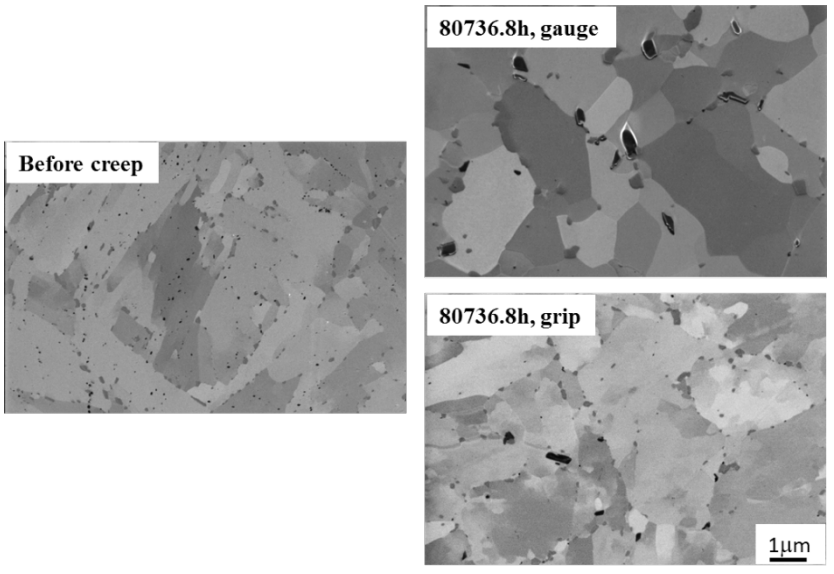

Figure 10 : SEM micrographs before and after creep.

Change in deformation resistance during creep

The relationship between the total number density of particles and creep time is shown in Fig.11. The total number density gradually decreased with increasing creep time in the grip and gauge portions. The total number density abruptly dropped after 50000h in the gauge portion as compared with the grip portion. The abrupt decrease in the total number density is due to the acceleration effect of stress or strain on the $M_{23}C_6$ coarsening, Z phase formation and disappearance of MX particles as shown in Fig.7 and Fig.9.

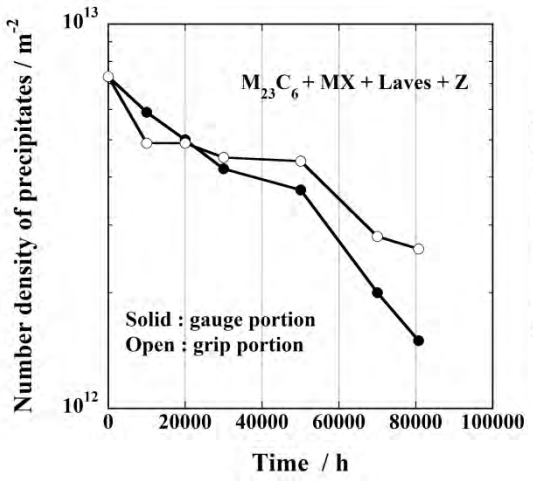

Figure 11 : Change in total number density of particles during creep.

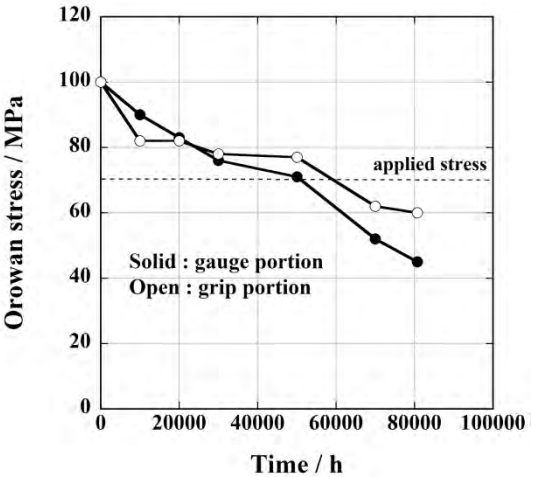

Figure 12 : Change in Orowan stress during creep.

Orowan stress σ_{Or} can be roughly described as follows.

$$\sigma_{Or} = 0.8MGb / \lambda \qquad (2)$$

where M, G, b and λ are the Taylor factor (=3), the shear modulus, the length of Burgers vector and inter-particle spacing, respectively. The inter-particle spacing of all particles including $M_{23}C_6$, MX, Laves phase and Z phase can be expressed by the total number density of particles *N* as follows.

$$\lambda = 1 / \sqrt{N} \qquad (3)$$

Orowan stress was estimated by the eq. (2) and (3). Figure 12 shows the change in Orowan stress during creep. Orowan stress gradually decreased with increasing creep time in the grip and gauge portions. In the gauge portion, Orowan stress rapidly dropped after 50000h as compared with the grip portion. Orowan stress after creep rupture was lower than the half value of initial Orowan stress in the gauge portion. The applied stress was 70MPa for the creep interrupted tests. Orowan stress is higher than the applied stress up to 50000h as shown in Fig.12. Orowan stress becomes lower than the applied stress after 50000h, indicating that the specimen can rapidly be broken after 50000h. However, it took about 30000h to reach creep rupture after 50000h. Therefore, it is difficult to discuss degradation mechanism by the change in Orowan stress during creep. The lath and block boundaries can contribute to strengthening [12]. It is needed for the degradation mechanism to consider both particle strengthening and boundary strengthening [13].

CONCLUSIONS

The stress or strain effect on microstructural changes during creep was investigated in T91 steel, focusing on the microstructure in the grip and gauge portions of crept samples. The results are summarized as follows.

1. The subgrain size gradually increased during creep in the grip and gauge portions. The subgrain size rapidly increased after 70000h in the gauge portion as compared with the grip portion. The dislocation density inside lath gradually decreased with increasing creep time in the grip and gauge portions. The dislocation density abruptly decreased after 70000h in the gauge portion.
2. The $M_{23}C_6$ size gradually increased during creep in the grip and gauge portions. The $M_{23}C_6$ size rapidly increased after 50000h in the gauge portion as compared with the grip portion. Ostwald-ripening equation could not explain the $M_{23}C_6$ coarsening in the gauge portion.
3. The Z phase was observed after creep in the grip and gauge portions. The number of Z phase particles was higher in the gauge portion than in the grip portion. The number of MX particles was lower in the gauge portion than in the grip portion.
4. The total number density of particles including $M_{23}C_6$, MX, Laves phase and Z phase was evaluated. The total number density gradually decreased during creep in the grip and gauge portions. The total number density rapidly decreased after 50000h in the gauge portion as compared with the grip portion.
5. Orowan stress was estimated from the total number density of particles. Orowan stress gradually decreased during creep in the grip and gauge portions. Orowan stress was higher than applied stress up to 50000h. However, Orowan stress abruptly decreased after 50000h in the gauge portion as compared with the applied stress.

REFERENCES

[1] H. Kushima, K. Kimura, F. Abe, Tetsu-to-Hagane 85 (1999) pp.841-847.
[2] K. Kimura, Proc. PVP2012-78323, 2012 ASME Pressure Vessels and Piping Division Conference, Toronto, Ontario, Canada July 15-19, 2012.
[3] K. Sawada, H. Kushima, T. Hara, M. Tabuchi, K. Kimura, Mater. Sci. Eng. A597 (2014) pp.164-170.
[4] K. Sawada, H. Kushima, M. Tabuchi, K. Kimura, Mater. Sci. Eng. A528 (2011) 5511-5518.
[5] K. Sawada, K. Maruyama, Y. Hasegawa, T. Muraki, Key Eng. Mater. 171-174 (2000) pp.109-114.
[6] Y. Qin, G. Götz, W. Blum, Mater. Sci. Eng. A341 (2003) pp.211-215.
[7] J. Hald and L. Korcakova：ISIJ Int. 43 (2003) pp.420.
[8] S. Spigarelli, E. Cerri, P. Bianchi and E. Evangelista：Mater. Sci. Tech. 15 (1999) pp.1433.
[9] F. Abe：Proc. The fourth Int. Conf. on Recrystallization and Related Phenomena, The Japan Institute of Metals, Sendai, (1999) pp.289.
[10] M. Taneike, M. Kondo, T. Morimoto, ISIJ Int. 41 (2001) pp.S111-S115.
[11] K. Sawada, H. Kushima, M. Tabuchi, K. Kimura, Mater. Sci. Tech. 30 (2014) pp.12-16.
[12] M. Mitsuhara, S. Yamasaki, M. Miake, H. Nakashima, M. Nishida, J. Kusumoto, A. Kanaya, Phil. Mag. Let. 96 (2016) pp.76-83.
[13] K. Maruyama, K. Sawada, J. Koike, ISIJ Int. 41 (2001) pp.641-653.